INTERNATIONAL JOURNAL OF HYDROGEN ENERGY 33 (2008) 5571–5582

Available at www.sciencedirect.com

ScienceDirect

journal homepage: www.elsevier.com/locate/he

Hydrogen production from ethanol steam reforming: energy efficiency analysis of traditional and membrane processes

G. Manzolini[a], S. Tosti[b,*]

[a]Politecnico di Milano, Dip. Energia, Piazza Leonardo da Vinci 32, Milano, Italy
[b]ENEA, Dip. FPN, C.R. ENEA Frascati, Via E. Fermi 45, Frascati, Roma I-00044, Italy

ARTICLE INFO

Article history:
Received 16 April 2008
Received in revised form
17 June 2008
Accepted 18 June 2008
Available online 14 September 2008

Keywords:
Ethanol steam reforming
Membrane reactor
Energy efficiency

ABSTRACT

The ethanol steam reforming reaction has been considered for producing pure hydrogen to be used for feeding a PEM fuel cell of power 4 kW. As an innovative technology, Pd–Ag thin wall membranes are proposed for building membrane reactors: accordingly, the energy efficiency analysis of the processes producing hydrogen from ethanol steam reforming has been carried out and, particularly, the comparison among a traditional process and different membrane processes is reported.

The traditional process studied consists of an ethanol reformer followed by two water gas shift reactors operating at high and low temperature, respectively: the final hydrogen purification is carried out by a preferential oxidizer in order to reduce the CO concentration below 10 ppm before feeding the PEM fuel cell.

Then two membrane processes using Pd–Ag tubes and operating with a feed H_2O/ethanol have been considered. The first one uses a traditional ethanol reformer and a Pd–Ag membrane reactor where the water gas shift reaction and the hydrogen separation simultaneously take place: the pure hydrogen recovered in the permeate side of the membrane reactor is sent to the PEM anode. In the second membrane process, one Pd–Ag membrane reactor performs the ethanol steam reforming with the hydrogen separation: also in this case, the pure hydrogen recovered in the permeate side of the membrane reactor is directly sent to the PEM anode.

The analysis showed that the highest values of the energy efficiency have been attained by the process using one membrane reformer: this process has a net electric efficiency of 9% higher than the traditional one.

Finally, an efficiency field-to-wheel analysis has been also carried out: a conventional application of the pure bio-ethanol in a reciprocating engine has been compared to a membrane system processing humid bio-ethanol and fuelling a PEM driven electrical engine. Mainly as a consequence of the direct use of water–ethanol mixtures, the membrane process presents a higher energy efficiency up to 50% and, in fact, in this case the distillation and dehydration of the bio-ethanol are avoided thus increasing the energy efficiency.

* *Corresponding author.*
E-mail address: tosti@frascati.enea.it (S. Tosti).

0360-3199/$ – see front matter
doi:10.1016/j.ijhydene.2008.06.029

Nomenclature

A	permeation surface area [m^2]
AC	alternating current
CWI	cathode water injection
DC	direct current
E_a	permeability activation energy [$J\,mol^{-1}$]
EFCV	electric fuel cell vehicle
F	Faraday's constant (96 439 $C\,mol^{-1}$ of electrons)
HE	heat exchanger
HRF	hydrogen recovery factor (Eq. (6))
i	cell stack current density [$A\,cm^{-2}$]
J	hydrogen molar flow rate across the Pd–Ag membrane [$mol\,s^{-1}$](Eq. (4))
LHV	low heating value ($MJ\,kg^{-1}$)
MREF	membrane steam reformer
n	pressure exponent depending on the permeation mechanism (Eq. (4))
Pe	Hydrogen permeability [$m^3\,m^{-1}\,s^{-1}\,Pa^{-0.5}$]
Pe_0	permeability pre-exponential factor (Eq. (5)) [$m^3\,m^{-1}\,s^{-1}\,Pa^{-0.5}$]
PEM	polymer electrolyte membrane fuel cell
p_F	hydrogen partial pressure at the Pd–Ag membrane feed side [Pa]
p_P	Hydrogen partial pressure at the Pd–Ag membrane permeate side [Pa]
PROX	preferential oxidizer
R	universal gas constant (8314 $J\,mol^{-1}\,K^{-1}$)
S/C	steam-to-carbon ratio
SR	conventional steam reformer
d	membrane thickness [m]
T	temperature [°C or K]
U_a	cell air utilization factor: $U_a = O_{2,consumed}/O_{2,inlet}$
U_f	cell fuel utilization factor: $U_f = H_{2,consumed}/H_{2,inlet}$
V	cell voltage (V)
WGSR	water gas shift reactor
η_{el}	overall net electric efficiency (LHV base)

1. Introduction

The hydrogen separation and production is becoming a theme of growing interest due to the capability of the hydrogen to be a clean energy vector [1]: in particular, the use of fuels produced from biomasses, such as the ethanol, can be considered environmentally sustainable [2]. In fact, the CO_2 produced during the ethanol reforming is the same depleted by the plants and drawn from the environment via the chlorophyll synthesis: consequently, such a process may contribute to decrease the CO_2-emission in the atmosphere [3]. In particular, beside the reduction of the green-house gas emissions, the ethanol produced from grass or wood has also small aggregate environmental costs [4].

Recent studies [5–7] have shown that 1 L of bio-ethanol (LHV equal to 21.20 $MJ\,L^{-1}$) obtained from conventional large scale plants requires for its production an amount of energy equal to 19.16 $MJ\,L^{-1}$; by considering as energy output also 4.16 $MJ\,L^{-1}$ of ethanol including "Distillers Dried Grains and Solubles (DDGS)" to be used in animal nutrition, an energy content carbon free of 6.20 $MJ\,L^{-1}$ is resulting. As a matter of fact, the introduction of bio-ethanol as energy carrier could decrease the CO_2 emissions of about 30%.

A summary of energy consumptions for ethanol production in conventional large scale plants is shown in Table 1. Values are taken from literature [8].

The conventional processes for producing bio-ethanol are based on the fermentation of the biomasses and, in particular, from the starch or the sugar-based feedstock via well-known and widespread methods. The sugar solutions are then fermented into ethanol by a further process which requires a large amount of water: the final content of ethanol after fermentation is about 50%, while the remaining 50% consists of water.

In order to limit the CO_2 emissions, the bio-ethanol is mainly used as a fuel in reciprocating engines for transportation use. This technology is very well recognized and reliable: for an example, in Brazil the ethanol impact on the total energy demand is about 15%. It's usually mixed with gasoline in a molar ratio in a range between 15% and 85% and used in so-called dual-fuel engine. However, in order to be used as a fuel for automotive applications, the mixture of ethanol and gasoline has to be water-free [9]. In fact, the ethanol when mixed with water has a higher "freezing" temperature with consequent problems in the winter period. Moreover, the ethanol has a high solubility in water: it tends to separate into a water–ethanol phase thus involving an heterogeneous composition of the fuel and leading to the engine malfunctioning. Consequently, bio-ethanol distillation and dehydration processes are required: in particular, the energy consumptions related to the distillation and the dehydration of ethanol are about 3 $MJ\,L^{-1}$ corresponding to the 20% of the total amount of energy required for producing 1 L of ethanol. In other words, the use of humid bio-ethanol permits

Table 1 – Energy input/output for a conventional large scale ethanol production plant

Energy input [$MJ\,L^{-1}_{EtOH}$]	
Energy consumption for farming	11.33
Corn transport and storage	0.14
Water distribution auxiliaries	0.60
Thermal cons. for ethanol prod.	6.85
Fermentation	1.49
Distillation–dehydration	3.14
Other consumptions	2.20
Electric cons. for ethanol prod.	0.76
Fermentation	0.62
Distillation–dehydration	0.04
Other consumptions	0.10
Ethanol transportation	0.08
Total energy input	19.16
Energy output [$MJ\,L^{-1}_{EtOH}$]	
Ethanol energy content	21.20
Secondary energy output	4.16
Total energy output	25.36
Net energy value, NEV	6.20

to increase the renewable energy content from 30% to about 43%: similar conclusions have been reported in literature [10].

Today, a possible innovative application of hydrogen derived from the bio-ethanol could concern the fuel cells. Especially, Polymer Electrolyte Membrane fuel cells (PEM) take advantage of their higher electric efficiency conversion when compared to a conventional internal combustion engine with particular benefits when it is operated under a partial load. Moreover, such an application allows the direct use of humid bio-ethanol by avoiding the necessity of a distillation process: a consequent lower energy consumption and lower production costs are expected, while the higher energy consumption for transporting the humid bio-ethanol is negligible. Aside from the automotive applications, the bio-ethanol derived hydrogen could be used in PEM fuel cells operating into combined heat and power (CHP) systems thus involving further energy savings and reduced CO_2 emissions.

At the moment, the commercially available and reliable PEMs convert directly the hydrogen into electricity: a fuel processing unit is required in order to transfer the energy content of the ethanol into a hydrogen-rich stream with an extremely low carbon monoxide concentration in order to avoid the poisoning of the fuel cell membrane. Appropriately, the steam reforming and auto-thermal reforming are the reference technologies for the hydrogen production. Between these two solutions, the steam reforming guarantees a higher hydrogen production efficiency [11–13].

In this work, a traditional steam reforming process is compared to innovative membrane systems: in fact, in the last years the membrane technologies have been playing a central role in the separation processes as a consequence of their capability to operate in a continuous mode and to save energy [14–16]. Especially, when a membrane selectively permeable to a reaction product is coupled to a catalysed reactor, a new device called membrane reactor is introduced. Such an apparatus allows to attain reaction conversion values higher than traditional reactors: this behaviour, called shift effect, is a consequence of the continuous removal of such a reaction product through the membrane [16]. When a membrane reactor uses a dense metal membrane with an infinite selectivity to the hydrogen, both the production of pure hydrogen from dehydrogenation reactions and its separation can be obtained in the same device.

Via an innovative technique developed at ENEA Frascati laboratories, Pd–Ag thin wall tubes have been produced [17–19]: their complete hydrogen selectivity and durability has been demonstrated in long term tests [20]. For producing pure hydrogen feeding a PEM fuel cell, a process for the ethanol steam reforming which uses a multi tube Pd–Ag reactor has been studied [21]: the experimental tests aimed at demonstrating the reaction yields are going on, while the effect of the operating parameters on the energy efficiency and the process design optimization are the subject of the study presented in this work. Particularly, from the operating point of view, the steam to carbon ratio and the temperature affect significantly the reaction yield. When low temperatures and low steam to carbon ratios are adopted, the catalyst deactivation (as a consequence of the coke formation) takes place, while higher energy efficiencies are expected because of the reduced specific heats to be provided to the reformer feed stream.

This paper considers two fuel processor systems using Pd–Ag membrane tubes for producing pure hydrogen able to feed a PEM fuel cell of power 4 kW: a comparison in terms of energy efficiency with respect to a conventional ethanol steam reforming process is studied, too.

Finally, in order to show its advantage of using humid bio-ethanol, a membrane system processing humid bio-ethanol and fuelling a PEM driven electrical engine has been compared to a conventional application of the pure bio-ethanol in a reciprocating engine in a simplified field-to-wheel analysis.

2. Model description

The ethanol steam reforming is an endothermic catalysed reaction whose conversion increases with the temperature:

$$C_2H_5OH + H_2O \Leftrightarrow 2CO + 4H_2 \quad \Delta H_{298}\,k = 239.5\ kJ\ mol^{-1} \tag{1}$$

via the water gas shift reaction the CO is converted into CO_2 producing further hydrogen:

$$CO + H_2O \Leftrightarrow CO_2 + H_2 \quad \Delta H_{298}\,k = -41.2\ kJ\ mol^{-1} \tag{2}$$

then, the complete reaction is:

$$C_2H_5OH + 3H_2O \Leftrightarrow 2CO_2 + 6H_2 \quad \Delta H_{298}\,k = 157.1\ kJ\ mol^{-1} \tag{3}$$

The hydrogen production from ethanol steam reforming is favoured at high temperature: consequently, the conventional reformers usually work at about 800–850 °C.

The main hypothesis considered in this analysis are described below and resumed in Table 2.

2.1. *Main assumptions*

By considering the reaction (3), two moles of ethanol react with three moles of water: then, the stoichiometric steam to carbon (S/C) ratio for the complete steam reforming reaction is 1.5. However, conventional systems usually work under higher S/C ratios [11]. As main considerations, high values of the steam to carbon ratio:

- move the reaction at the product side,
- limit the carbon deposition on catalyst surface and
- increase the heat needed for evaporating the feed water with negative consequences on system efficiency.

The literature reports several works about the carbon deposition into conventional reformers: the results depend on the reaction temperature and the type of catalyst used. In practice, the minimum S/C ratio moves from 1.5 to 3 [22–24]. Low temperatures promote the carbon deposition: 600 °C can be considered the breakthrough temperature for S/C ratio higher than 1.5.

In this analysis, a S/C ratio at the reactor inlet equal to 3 has been considered as the reference case, being a compromise between the system efficiency and the carbon deposition.

All the reactions have been considered under thermodynamic equilibrium conditions (i.e., infinite reaction kinetic). The pressure drops through the catalyst bed of the reactors have been set equal for all the three cases, while the thermal

Table 2 – Simulation assumptions

Reformer	
Temperature (°C)	830
Inlet pressure (bar)	1.4
Pressure losses (%)	4.0
Thermal losses (as % of the heat required by reaction, %)	4.0
Water gas shift membrane reactor	
Temperature (°C)	350–450
Inlet pressure (bar)	6.0
Pressure losses (feed side, %)	4.0
Thermal losses (as % of the heat produced by reaction, %)	2.0
Membrane reformer	
Temperature (°C)	600
Inlet pressure (bar)	8.0
Pressure losses (feed side, %)	4.0
Thermal loss (as % of the heat required by reaction, %)	3.0
Heat exchangers	
ΔT pinch point for evaporator (°C)	13
Minimum ΔT for gas–liquid heat transfer (°C)	10
Pressure losses (%)	2.0
Thermal losses (referred to heat transferred, %)	1.0
Water gas shift reactor	
Pressure losses (%)	1.0
Thermal losses (as % of the heat produced, %)	2.0
PROX	
Pressure losses (%)	2.0
Thermal losses (as % of the heat produced, %)	1.0
Combustor	
Pressure losses (%)	4.0
Thermal losses (as % of the combustion heat, %)	3.0
O_2 concentration at the exhaust exit (%)	4.0
Compressors polytropic efficiency (%)	70
Pump electric and hydraulic efficiency (%)	72
Fuel cell	
Net electric power (W)	4000
Current density (mA cm^{-2})	250
Pressure drop, anode and cathode side (%)	1.0
Average working temperature (°C)	75
Electrical and auxiliaries efficiency	
DC/AC converter (%)	96.5
DC/DC converter (%)	97.8
Electrical motors (drivers, %)	4.05 ln(Power(kW)) + 43.2
Other auxiliary consumption (% of Net power)	1.0

losses differ because of the different working temperatures which affect the amount of heat released to the environment.

2.2. Pd–Ag membranes

The hydrogen interacts with the metals: in general, its uploading and diffusion into the metal lattice have been well described [25,26]. When a dense metal wall separates two gaseous phases, the mass transfer mechanism (i.e., the gas permeation) taking into consideration the absorption/diffusion of the hydrogen through the metal can be expressed by the Sieverts' law:

$$J = \frac{\mathrm{Pe}}{d}\left(\sqrt{p_\mathrm{F}} - \sqrt{p_\mathrm{P}}\right)A \quad (4)$$

where Pe is the hydrogen permeability, [m^3 m^{-1} s^{-1} Pa$^{-0.5}$], J is the hydrogen permeating flow rate, [m^3 s^{-1}], d is the membrane (tube) thickness, [m], p_F is the hydrogen partial pressure in the feed side of the membrane, [Pa], p_P is the hydrogen partial pressure in the permeate side, [Pa], A is the permeation surface area, [m^2].

Furthermore, an Arrhenius law gives the dependence of the hydrogen permeability vs. the temperature:

$$Pe = \mathrm{Pe}_0 e^{-E_\mathrm{a}/RT} \quad (5)$$

where Pe_0 is the pre-exponential factor, [m^3 m^{-1} s^{-1} Pa$^{-0.5}$], E_a is the apparent activation energy factor, [J mol^{-1}], R is the gas constant, [J mol^{-1} K^{-1}], T is the absolute temperature, [K].

As a consequence of their high hydrogen permeability, the Pd and its alloys are used to build dense permeators able to separate selectively the hydrogen from gaseous mixtures. Especially, the Pd–Ag alloy with silver content 23–25%wt. is commercially used to produce permeator tubes of wall thickness 0.100–0.150 mm.

In this work, thinner and cheaper Pd–Ag tubes of diameter 10 mm and wall thickness 0.050 mm produced via cold-rolling and diffusion welding have been considered [18]. On the basis of previous experimental works, the following values of the hydrogen permeability coefficients have been taken into account:

$$\mathrm{Pe}_0 = 1.09 \times 10^{-8} \quad \left[\mathrm{m^3\ m^{-1}\ s^{-1}\ Pa^{-0.5}}\right]$$

$$E_\mathrm{a}/R = 2566.0 \quad [K]$$

Particularly, these thin wall Pd–Ag permeator tubes have been experienced in the temperature range 300–400 °C and with transmembrane pressure up to 200 kPa. For applications considered in this work, the membranes operate under more severe conditions: temperatures of 600 °C and transmembrane pressure up to 600 kPa. Under such conditions, the availability of these Pd–Ag membranes could be guaranteed by the application of special strengthening metal supports as previously investigated [27].

2.3. Energy and mass balances

The energy and mass balances of the fuel processor systems have been estimated by a modular simulation code originally developed to assess the performance of gas/steam cycles for power production [28–31]: such a code has been then extended to high temperature fuel cells [32,33], PEM fuel cells and membrane reformers [34,35].

2.4. Polymer electrolyte membrane fuel cell

The PEM performance has been computed starting from the polarization curve proposed reported in literature [36] and verified in a previous calibration campaign [37]. The polarization curve considered gives a cell voltage of 0.784 and 0.698 V for current density of 250 and 600 mA cm^{-2},

respectively. When the PEM is fed with reformate gases as in the SR cases, the cell voltage decreases to 0.738 V at current density of 250 mA cm^{-2} as a consequence of the higher activation losses due to the presence of inert gases [38].

These PEM working conditions are typical of modern PEM fuel cells applied to high efficiency micro-cogenerative systems where the dimension and the weight are not important requirements [37,39].

2.5. *Electric devices and auxiliaries*

To increase the PEM voltage, the electric connections require a DC/DC converter with integrated electronic inverters and AC electric drivers for auxiliary pumps and compressors. The electric drivers efficiency has been considered as a function of the nominal net power (kW) by a logarithm law as reported in Table 2.

The net power output has been considered at 230 V in AC as in the typical CHP systems. In the case of automotive applications, the electronic connection can be further optimized (i.e., by introducing an auxiliary battery).

3. Conventional steam reformer process (SR-P)

The ethanol conversion into hydrogen is generally performed with a good efficiency by a steam reforming reactor which requires the presence of water to sustain the reforming process. As a matter of fact, a part of the water necessary to the steam reforming reaction is already present in the humid bio-ethanol.

The proposed process is shown in detail in Fig. 1, while Table 3 reports the characteristics of the process streams in terms of dimensionless mass flow rates and the compositions.

Accordingly to the scheme of Fig. 1 the water–ethanol mixture is pumped up to a pressure of 1.4 bar and pre-heated before entering the conventional fixed bed catalysed reformer (REF). The reformer works at 830 °C and about 1.35 bar, with an inlet S/C ratio equal to 3. As a consequence of the high temperature and low pressure, the conversion of ethanol is high, while the CO content of the exit stream is still relevant (see Table 3). In order to increase the hydrogen production and to reduce the CO content, the syngas generated by the steam reforming requires two further purification steps. The first one considers the water gas shift reaction carried out into two reactors separated by a cooling heat exchanger, while the second one consists of a preferential oxidizer. This technology is rather well-known and reliable, even if it requires several conversion steps affecting the net electric efficiency. Correspondingly, additional steam is added to the reformate stream for producing as much H_2 as possible from CO conversion into CO_2. This reaction is carried out into two water gas shift reactors: a first water gas shift reactor operating at high temperature (WGS HT) and a second one operating at low temperature (WGS LT).

The S/C ratio of the stream entering the WGS HT is equal to 3.5; the water gas shift reaction is exothermic, hence a cooling step is introduced to increase the reaction yield. After the WGS LT, a preferential oxidizer (PROX) decreases the CO content of the stream below 10 ppm, a typical tolerance limit of the PEM. In this reactor the CO is burned with air in presence of a catalyst that inhibits the hydrogen combustion: accordingly, the final composition of the fuel at the anode inlet mainly consists of water saturated H_2 and CO_2, see the stream 5 of Table 3.

Consequently, the stream leaving the PEM anode (stream 9 of Table 3) contains a hydrogen concentration as high as sufficient to limit the voltage losses at the anode side: as a result, only a part of H_2 can be converted into electricity. For this reason, the fuel utilization (U_f) has been taken equal to 0.75 [37]. In particular, the stream leaving the anode is composed by the unused hydrogen, CO_2 and steam; the residual heating value of the mixture, with an addition of ethanol, is exploited in a burner to sustain the heat demand of the reforming reaction. The amount of air required for the

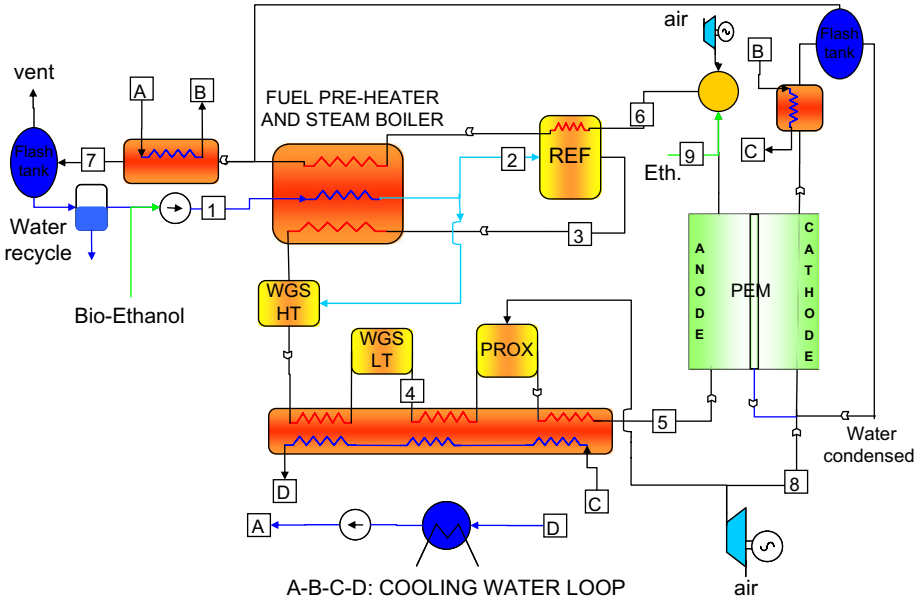

Fig. 1 – Schematic representation of the PEM system based on a conventional fuel processor (REF).

Table 3 – Stream data for a system based on a conventional fuel processor REF (Fig. 1)

Point #	T (°C)	P (bar)	M (–)	Eth.	CO	CO_2	H_2	H_2O	O_2		Inerts
									Humid	Dry	
1	15.0	1.42	1.00	14.3				85.7			
2	600.0	1.40	1.00	14.3				85.7			
3	830.0	1.37	1.00	0.1	9.0	9.10	45.3	36.5			
4	212.8	1.30	1.35	0.04	0.1	14.2	42.7	43.0			
5	70.0	1.20	1.12	0.1	0.00	16.8	49.6	32.5			1.2
6	1228.5	1.04	3.29			14.9		27.5	4.0	5.5	53.0
7	30.0	1.10	3.29			14.9		27.5	4.0	5.5	53.0
8	15.0	1.10	0.15	50.00				50.0			
9	35.7	1.20	4.03					1.0	20.73	21.0	78.2

The mass flow rates M are dimensionless values related to the ethanol stream entering the reformer (M = 1), while the compositions of the reactants and the products are reported as molar concentration (%).

combustion is calculated in order to have an oxygen concentration humid volume at the combustor outlet set to 4%.

The temperature of the vented exhaust gases is about 210 °C, a rather high value influenced by the pinch point conditions required by the heat exchange process occurring in the reformer.

The PEM fuel cell is humidified by the direct water injection at the cathode (CWI) [40], without requiring any additional humidification at the anode side. In this particular case, the stream at the anode inlet is water saturated as a consequence of the hydrogen production process. The PEM average working conditions are 1.2 bar and 75 °C.

4. Membrane fuel processors

In the following analysis, membrane reactors consisting of a bundle of Pd–Ag tubes have been considered for studying the innovative fuel processors: in particular, two processes have been evaluated:

- a traditional fixed bed ethanol reformer (REF) followed by a Pd–Ag membrane reactor where the water gas shift reaction takes place (WGSMR) and
- one Pd–Ag membrane reactor carrying out the ethanol steam reforming (MREF).

A schematic representation of the two membrane reactors performing the water gas shift reaction and the ethanol reforming are shown in the Fig. 2. In both cases, each tubular membrane has a dead-end configuration: this design allows lower mechanical stresses of the thin wall tubes due to the thermal and hydrogenation cycling of the palladium alloy [21].

The membrane reformer arrangement is more complicated than the water gas shift one: in fact, the ethanol steam reforming is an endothermic reaction and high temperature gases are required in order to provide the reaction heat through an appropriate heat exchanging system. In particular, the temperature in the MREF is assumed to be constant (the heat supplied by the hot gases is equal to the reforming heat demand), while in the WGSMR the heat released by the reaction increases the temperature all along the membrane surface area with a maximum ΔT of about 50 °C.

In the two membrane processes considered, a membrane reactor produces a pure hydrogen stream feeding the PEM fuel cell by operating in a dead-end configuration with a fuel utilization reaching 100%. In fact, all the hydrogen produced is converted into electricity thus limiting the fuel losses.

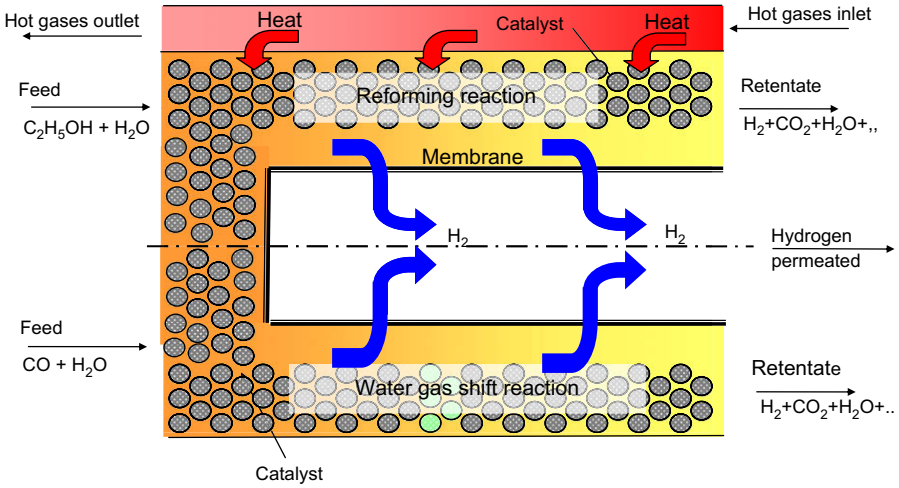

Fig. 2 – Conceptual scheme of (upper part) ethanol membrane reformer and (lower part) the water gas shift membrane reactor.

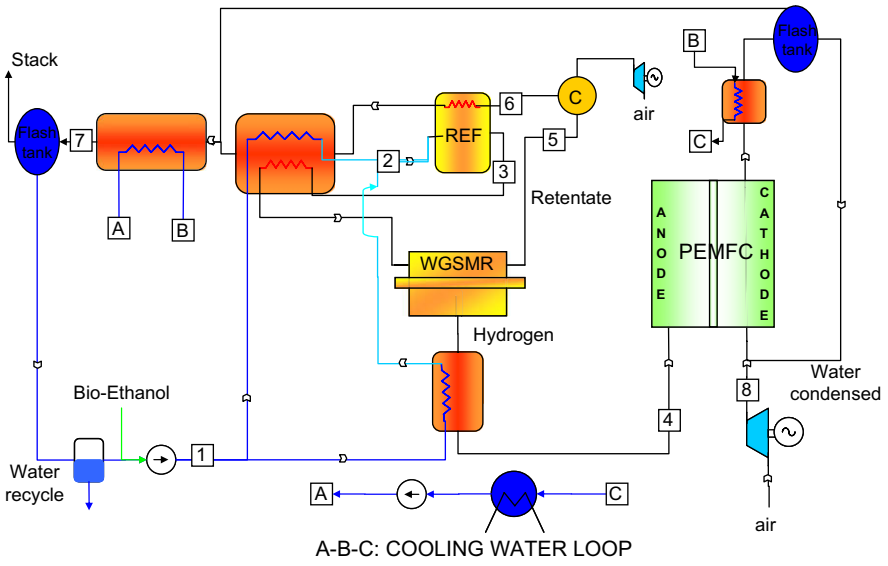

Fig. 3 – Schematic representation of the PEM system based on a water gas shift membrane reactor (WGSMR).

Moreover, when the fuel cell is fed with pure or humidified hydrogen (undiluted by inert species), large benefits are attained in terms of electric conversion efficiency: in fact, at the same current density, a higher Nernst potential and a higher cell voltage are achieved with respect to the reformate fuels.

A typical parameter to describe the membrane reactor performance is the Hydrogen Recovery Factor (HRF): it gives information about the hydrogen separated in the reactor with respect to the maximum amount that can theoretically be separated assuming an infinite membrane surface area. Appropriately, by taking into account also the hydrogen formed by the reaction occurring in the water gas shift membrane reactor, the following expression can be defined:

$$\mathrm{HRF} = \frac{n_{\mathrm{H_2,separated}}}{n_{\mathrm{H_2,max}}} = \frac{n_{\mathrm{H_2,separated}}}{n_{\mathrm{H_2,in}} + n_{\mathrm{CO,in}}} \tag{6}$$

where $n_{\mathrm{H_2,separated}}$ refers to the number of hydrogen moles separated through the membranes, while $n_{\mathrm{H_2,in}}$ and $n_{\mathrm{CO,in}}$ indicate the moles of hydrogen and carbon dioxide at the inlet of the reactor, respectively.

When the steam reforming reaction takes place in the membrane reactor, the previous formula is modified. In this case, accordingly to the expression (3), the denominator has to take into consideration the moles of ethanol fed multiplied by the stoichiometric coefficient 6 instead of the moles of CO and H_2:

$$\mathrm{HRF} = \frac{n_{\mathrm{H_2,separated}}}{n_{\mathrm{H_2,max}}} = \frac{n_{\mathrm{H_2,separated}}}{6 \times n_{\mathrm{C_2H_5OH,in}}} \tag{7}$$

4.1. *Water gas shift Pd–Ag membrane reactor process (WGSMR-P)*

This process is still based on a conventional reformer, but the hydrogen is produced and purified in a membrane reactor performing the water gas shift reaction. Compared to the previous case, two reactors are present instead of four: see Fig. 3 for the process scheme and Table 4 for the dimensionless mass flow rates and the compositions of the process streams. This solution increases the hydrogen production efficiency as well as produces in the permeate side of the Pd–Ag membrane

Table 4 – Stream data for a system based on the WGSMR (Fig. 3)

Point #	T (°C)	P (bar)	M (–)	Eth.	CO	CO_2	H_2	H_2O	O_2		Inerts
									Humid	Dry	
1	15.0	6.35	1.00	14.29				85.71			
2	450.0	6.23	1.00	14.29				85.71			
3	780.0	6.00	1.00	0.68	8.84	8.91	43.73	37.84			
4	75.0	1.20	0.05				100.00				
5	447.6	5.92	0.95	1.03	1.85	25.17	25.99	45.97			
6	1216.5	1.05	0.25			13.89		37.21	4.00	6.37	44.90
7	30.0	1.01	0.25			13.89		37.21	4.00	6.37	44.90
8	35.7	1.20	0.34					1.03	20.73		78.23

The mass flow rates M are dimensionless values related to the ethanol stream entering the reformer (M = 1), while the compositions of the reactants and the products are reported as molar concentration (%).

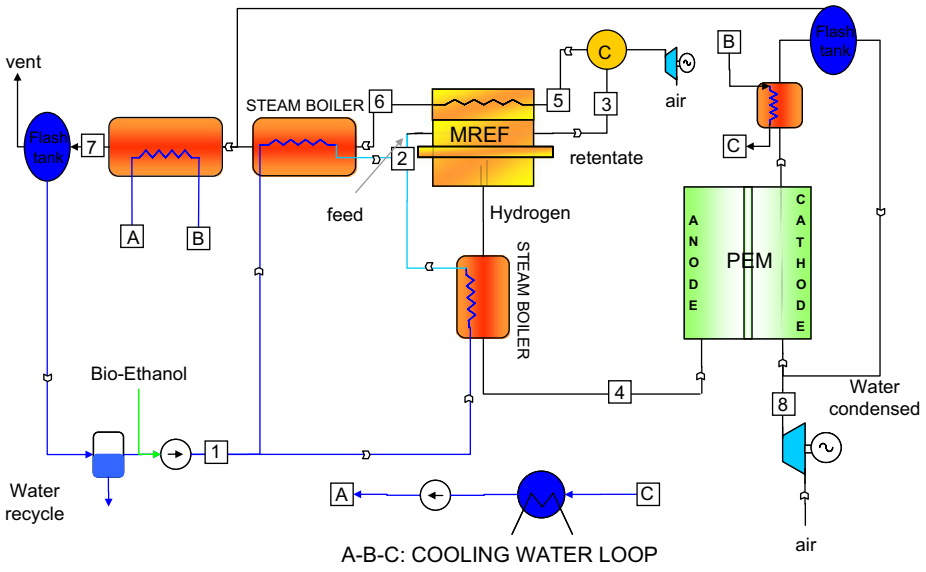

Fig. 4 – Schematic representation of the PEM system based on a membrane reformer (MREF).

reactor a pure hydrogen stream to be sent to the anode of the PEM where it is completely converted.

Also in this case, the steam reformer works with a S/C of 3, while a lower temperature (about 780 °C) is adopted. The reformate stream is cooled at 350 °C and sent to the WGSMR: such a temperature has been taken in order to limit the poisoning effect of CO on the palladium alloy membranes [41,42].

In order to promote the hydrogen permeation across the membrane and thus limiting the membrane surface area, the feed and permeate pressures have been set equal to 6.0 and 1.22 bar, respectively. Compared to SR-P, the higher pressure has negligible consequences on the auxiliaries power demand (i.e., the pumps): on the contrary, it significantly increases the evaporation temperature of ethanol–water mixture. No addition of steam to the WGSMR feed stream is carried out: in fact, a higher water vapour partial pressure could reduce the hydrogen partial pressure in the feed side of the membranes, thus reducing the hydrogen permeation driving force. After cooling, the ultra-pure hydrogen separated in the lumen side can be directly sent to PEM and converted into electricity: the fuel cell works in a dead-end configuration with an U_f equal to 1.

Accordingly to formula (6), the HRF considered in this assessment is set at about 69% in order to avoid any addition of fuel. The combustion of the retentate stream (composed of hydrogen, ethanol and unconverted carbon monoxide) provides the exact amount of heat required by the reformer and the pre-reforming section without any need of additional fuel.

4.2. *Pd–Ag membrane reformer process (MREF-P)*

The application of the ethanol Pd–Ag membrane reformer results in a compact scheme, as it is presented in the Fig. 4. The dimensionless mass flow rates and compositions of the process streams are reported in the Table 5.

In this process, the hydrogen production and separation take simultaneously place in one reactor: the membrane reformer (MREF). A mixture of ethanol and water with a S/C equal to 3, after evaporation and pre-heating at a temperature of 600 °C, is directly sent to the MREF. Reforming temperatures

Table 5 – Stream data for a system based on the MREF (Fig. 4)

Point #	T (°C)	P (bar)	M (–)	Eth.	CO	CO_2	H_2	H_2O	O_2		Inerts
									Humid	Dry	
1	15.0	8.10	1.00	14.3				85.7			
2	450.0	8.00	1.00	14.3				85.7			
3	600.0	7.70	1.00	2.9	2.9	24.0	17.1	53.2			
4	75.0	1.20	0.05				100.0				
5	1226.1	1.07	2.40			14.5		37.8	4.0	6.4	43.7
6	911.8	1.05	2.40			14.5		37.8	4.0	6.4	43.7
7	30.0	1.01	2.40			14.5		37.8	4.0	6.4	43.7
8	35.7	1.20	3.51					1.3	20.7		78.2

The mass flow rates M are dimensionless values related to the ethanol stream entering the reformer (M = 1), while the compositions of the reactants and the products are reported as molar concentration (%).

higher than 600 °C could reduce the membrane stability as a consequence of the Ag evaporation from the Pd alloy, while the adopted transmembrane pressure is a compromise between the required membrane surface area and the system efficiency. The pressure of the feed side has been set equal to 8.0 bar with a permeate pressure of 1.22 bar. These selected pressures have been chosen as a compromise taking into consideration the resulting membrane surface area and the system efficiency. In fact, higher pressures increase the hydrogen permeation flux across the membrane thus limiting the membrane surface area but rise the evaporation temperature of the feed stream thus reducing the system efficiency. As a consequence, a higher evaporation temperature increases the exhaust gases temperature and, consequently, the heat released to the ambient.

In this case, the HRF has been calculated with reference to the expression (7) and set to the value 64.8%: as a matter of fact, any additional input of fuel for providing the reaction heat is needed. As in the previous case, after cooling, the hydrogen collected in the membrane reactor is directly sent to the PEM operated in a dead-end mode.

5. Results and discussion

The energy efficiency analysis of the conventional ethanol steam reforming process and the two fuel processor systems using the Pd–Ag membrane tubes has been carried out by considering the production of hydrogen feeding a PEM fuel cell of power 4 kW. Particular attention has been given to the influence of the S/C ratio and the current density.

Further, in order to emphasize the advantages of using a membrane system processing humid bio-ethanol and fuelling a PEM driven electrical engine with respect to a conventional application of the pure bio-ethanol in a reciprocating engine, a field-to-wheel analysis has been also performed.

5.1. *Comparison of the traditional and membranes processes*

An important consideration concerns the different values of the reforming temperature adopted for the three processes studied in this work. In the traditional process (SR-P), the temperature of 830 °C has been adopted with reference to the most of applications [11–13,38]: in fact, a lower ethanol steam reforming temperature decreases the ethanol conversion thus involving also a reduced hydrogen partial pressure at the PEM inlet, with negative consequences on the cell voltage and the overall system efficiency. On the other hand, when a WGSMR is used for completing both the CO conversion and the hydrogen separation (WGSMR-P case), the amount of ethanol converted in the SR-P affects only the partial pressure of the hydrogen entering the WGSMR (i.e., only the Pd–Ag membrane area). In this case, thanks to the Pd–Ag membranes, only pure hydrogen is sent to the PEM anode thus avoiding any cell voltage drop. By considering that the retentate energy content is the exact amount required by the reforming reaction and pre-heating section, a lower ethanol conversion doesn't significantly affect the overall system efficiency, so that the reformer temperature can be set at 780 °C in order to limit the heat losses. Finally, for the MREF-P the temperature of 600 °C has been adopted: in fact, over such a temperature the Pd–Ag membranes stability could be reduced.

Table 6 – Energy balances for the three processes studied (figures in brackets refer to the electric losses of the element)

	SR-P	WGSMR-P	MREF-P
Pd–Ag membrane surface area, m^2	–	1.19	0.89
PEM active are, m^2	2.43	2.28	2.28
FC power output, W	4483	4467	4476
DC/DC conversion losses, W	100	100	100
Net FC power DC, W	4383	4366	4376
Cathode compressor, W	157 (65)	148 (62)	147 (62)
Combustor compressor, W	16 (8)	16 (8)	26 (13)
Pump consumptions, W	24 (13)	17 (9)	17 (9)
Auxiliaries, W		40	
Net power at inverter input, W		4146	
DC/AC conversion losses, W		146	
Net electrical power, W		4000	
Reforming bio-ethanol, W	9090	10130	9292
Additional bio-ethanol, W	3246	–	–
Total power input (LHV), W	12336	10130	9292
Net electric efficiency (LHV), %	32.43	39.48	41.18

The energy balances of the three processes described in detail in the above section have produced the results shown in the Table 6. The net electric power output has been set equal to 4 kW for each case: this has been obtained by changing the amount of the bio-ethanol fed at the inlet of the system. The fuel cell power output is almost the same for all three cases because of the slightly different auxiliary consumptions. The most significant difference could be related to the combustor compressor work in the MREF-P case and the pump consumptions for the SR-P. In fact, it has been assumed that the pressure losses of the hot gases in the MREF are higher than the conventional reformer ones as consequence of the more complicated MREF arrangement. On the other hand, for the SR-P the pumps consumptions power are higher because of the more complex coolant loop required: as a result, these two aspects well balance each other.

With a S/C of 3, the net electric efficiency for the conventional fuel processor is 32.43%, close to the value calculated in a previous work [43]. The second (WGSMR-P) and the third case (MREF-P) considered achieve an efficiency higher of about 7%, and 9% than the SR-P case, respectively. The lower efficiency of the conventional case compared to the innovative membrane ones is mainly due both to the lower hydrogen production efficiency and the lower PEM fuel cell voltage consequent to the hydrogen dilution. In the SR-P, the hydrogen conversion efficiency in the fuel cell is about 5% lower compared to PEM fed with pure hydrogen.

The WGSMR-P and MREF-P have the same fuel cell efficiency (i.e., the fuel cell operating conditions are equal in terms of feed stream, temperature and pressure), thus the difference of 1.7% of the overall electric efficiency is only related to the fuel processing scheme: from the energy balance point of view, the presence of two reactors in the WGSMR-P instead of one in the MREF-P significantly affects the electric efficiency.

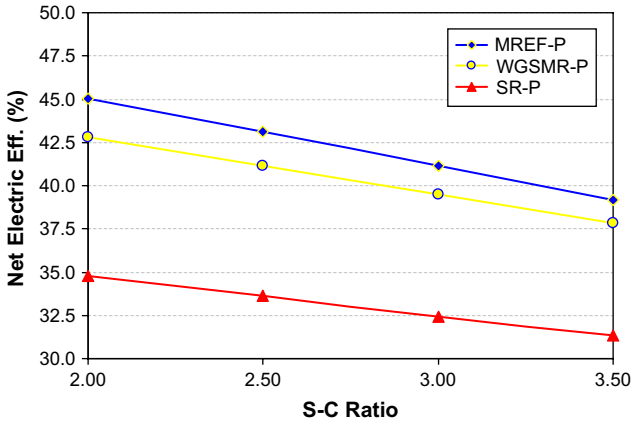

Fig. 5 – S/C ratio sensitivity analysis: the net electric efficiency for the conventional fuel processor (SR-P), the conventional steam reformer with the water gas shift membrane reactor (WGSMR-P) and the membrane reformer (MREF-P).

As another remark, the two membrane processes (WGSMR-P and MREF-P) have the same PEM active area because of the same PEM efficiency and the similar system power output, while Pd–Ag membrane surface area is significantly higher for WGSMR due to the lower working temperature that significantly influences the hydrogen permeability (see Eq. (5)).

The S/C ratio of the reformer feed stream is a key parameter for optimizing such systems: in fact, it strongly affects the system efficiency. Furthermore, low S/C ratios could involve the carbon deposition on the steam reforming catalyst. For these reasons, a sensitivity analysis of this parameter has been carried out in the S/C range from 2 to 3.5: the results are shown in Fig. 5. By reducing the S/C ratio from 3.5 to 2, which is considered the minimum value to avoid carbon deposition, the net electric efficiency increases more than 5 percentage points for the two innovative membrane processes, while the process using the conventional reformer shows a slightly efficiency increase.

The influence of the S/C ratio on the system electric efficiency can be understand by analysing the heat transfer

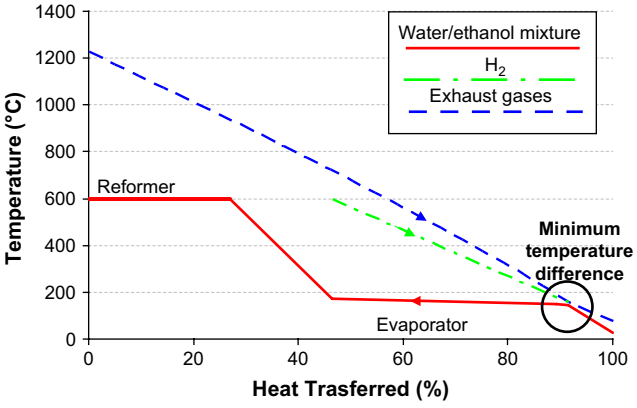

Fig. 6 – Temperature profiles of the exhaust gases and the water–ethanol mixture vs. the heat transferred for the MREF.

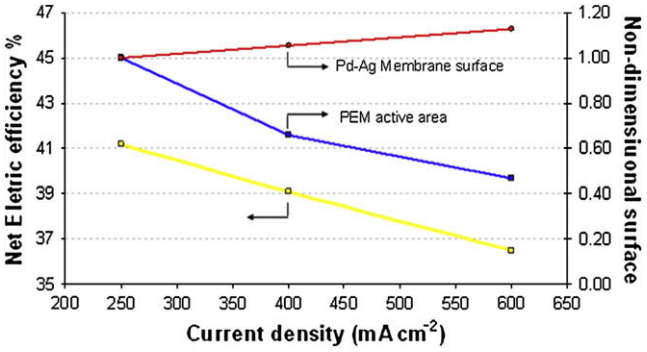

Fig. 7 – Membrane reformer fuel processor (MREF-P) case carried out with a S/C ratio of 3. The net electric efficiency, the PEM active area and the membrane surface vs. the current density.

profiles between exhaust gases and water–ethanol mixture (see Fig. 6).

For the two membrane systems, the minimum temperature difference (pinch point) in the heat exchange is on the evaporator so that the amount of water in the stream largely affects the heat required for its evaporation. Thus, when a higher S/C ratio is adopted there is a higher heat demand in the fuel processor by leading to a lower hydrogen separation in the membrane reformer as well as a lower net electric efficiency. Otherwise, in the SR-P the pinch point is located on the steam reformer, so that the heat required by the whole fuel processor mainly depends on the heat supplied to the reformer itself. Then, the amount of steam has a small influence on the ethanol conversion in the reformer: a higher S/C ratio lightly increases the ethanol converted and consequently the global heat required.

The energy balances have been calculated with a low value of the current density by considering the use of a PEM fuel cell characterized by high conversion efficiencies rather than limited dimensions and weight: correspondingly, a PEM current density of 250 mA cm^{-2} has been used [42]. Furthermore, the PEM current density affects significantly the PEM active area and the costs beside the electric efficiency. Therefore, a parametric analysis has been carried out: the Fig. 7 shows the results obtained for the membrane reformer fuel processor (MREF-P) case with a S/C ratio equal to 3. The corresponding efficiency for other cases or different S/C ratios can be approximately extrapolated by applying, at a current density of 250 mA cm^{-2} of the Fig. 7, the efficiency proposed in Fig. 5 and maintaining constant the slope of the line depicted in the example proposed.

As it results from the Fig. 7, by increasing the current density to 600 mA cm^{-2}, the efficiency decays by about 5 percentage points; analogously, also the PEM active area reduces significantly. On the contrary, the Pd–Ag membrane surface area increases with the current density as a constant system power output has been assumed (4 kW): for a higher current density, the PEM efficiency decreases thus requiring more hydrogen. At the state of art, the most expensive part of these systems is the PEM: consequently, the process optimization could be lead by considering as a controlling parameter the cost of the fuel cell rather than Pd price.

5.2. *Field-to-wheel analysis*

Beside the high conversion efficiency, the ethanol reforming fuel processors allow the utilization of the humid bio-ethanol (a 50% molar water–ethanol mixture) with significant energy and cost saving in the bio-ethanol production processes. As minor drawbacks, the application of the humid bio-ethanol obviously introduces fuel freezing problems and reduces the vehicle autonomy because of the lower energy content per volume unit.

The net energy conversion of bio-ethanol for the utilization in an automotive application is studied in this section. The simplified field-to-wheel energy considered in this study is the net energy obtained from the bio-ethanol utilization starting from the harvest until the conversion into the mechanical energy: Table 1 showed in details the energy consumption from the harvest to the production and distribution.

In this analysis three systems have been considered: the use of pure bio-ethanol in a reciprocating engine of 50 kW maximum power output and two membrane reformers (MREF-P) using a 50% water–ethanol mixture and producing pure hydrogen for feeding PEM fuel cells driving electrical engines. About the reciprocating engine, for simplicity an optimal working condition has been assumed corresponding to an efficiency of 36%: as a matter of fact, the part-load efficiency decay has been neglected.

For the recent proposed automotive applications, a typical range of the current density values are 250 and 600 mA cm^{-2}: in this field-to-wheel analysis the same PEM efficiency adopted for the 4 kW systems has been assumed without considering any scale-up effect. This is a conservative assumption: in fact, even if the PEM is a modular system and the efficiency doesn't depend on its size. In fact, at part-load the auxiliaries efficiency decreases while the PEM voltage increases: as a result, the PEM system efficiency is constant in a wide operative range. The other conversion efficiency values considered are the electric driver + control system (only for the MREF-P) and the mechanical transmission (for both the MREF-P and the RE) set at 90% and 98%, respectively.

The Table 7 shows the results of this analysis. When the bio-ethanol is used in the MREF-P systems, the field-to-wheel efficiency increases up to 50% compared to the conventional reciprocating engine application. Especially, the MREF-P systems use dilute bio-ethanol thus requiring minor energy for the fuel production: further, these systems are characterized by the higher efficiency of the fuel cell with respect to the reciprocating engine. The utilization of lower S/C ratio (for example 2.5 or below) can further increase the field-to-wheel efficiency.

Table 7 – Field-to-wheel balances for the ethanol application in a reciprocating engine and a MREF

	RE	MREF-P	
S/C ratio	–	3	
Current density, mA cm^{-2}		250	600
Ethanol energy content, MJ	100		
Bio-ethanol volume required, L	4.72	9.43	
Energy required for bio-ethanol production, MJ	70.75	55.75	
Transportation energy consumption, MJ	0.38	0.76	
Tank net energy, MJ	28.86	43.48	
Engine/FC efficiency, %	36.00	41.18	36.51
Electric driver + mechanical transmission, %	98.00	88.20	88.20
Global conversion efficiency, %	35.28	36.32	32.20
Net final energy, MJ	10.18	15.79	14.00

6. Conclusions

This paper investigates the application of the bio-ethanol for producing hydrogen in innovative systems where Pd-based membrane fuel processors and PEM fuel cells technologies are applied.

As a main result, these new systems allow the use of humid bio-ethanol: in this case the renewable energy content of the bio-fuel reaches about 43%, instead of the value of 30% of the pure bio-ethanol widely proposed into the conventional reciprocating engines. As a drawback, the membrane reactor/PEM fuel cell systems need a fuel processing unit in order to transfer the energy content of the ethanol into a hydrogen-rich gas stream to be converted into electricity in the fuel cell driving an electrical engine.

Three different fuel process systems have been compared: the first one based on a conventional high temperature steam reforming reactor and two membrane processes where a water gas shift and a steam reforming membrane reactor have been used, respectively. Dense Pd–Ag membrane tubes of wall thickness 50 μm have been studied for building the membrane reactor: as a consequence of their high hydrogen permeability and complete selectivity, pure hydrogen is produced to be used directly into the PEM anode.

Accordingly to the results of this study, the processes based on the water gas shift and the steam reformer membrane reactors yield net electrical efficiencies as high as 39% and 41%, respectively; these values are about 7% and 9% higher than the values obtained for the system based on the traditional ethanol reformer.

The steam to carbon ratio of the water–ethanol stream feeding the systems has been selected as a critical parameter affecting significantly the system efficiency: so, a sensitivity analysis based on such a parameter has been carried out. When low S/C ratio values are considered, the energy efficiency increases significantly, even if the carbon deposition on the catalyst with its consequent deactivation could take place thus reducing the system reliability and availability.

Finally, a simplified field-to-wheel analysis has been carried out: the energy efficiency increases up to 50%, when the membrane reactors are used coupled to PEM fuel cells driving electrical engines with respect to the use of conventional reciprocating engines. This result depends mainly on the use of innovative membrane systems capable to process the humid bio-ethanol.

REFERENCES

[1] Valenti G, Macchi E. Proposal of an innovative, high-efficiency, large-scale hydrogen liquefier. Int J Hydrogen Energy 2008;33:3116–21.

[2] Goltsov V, Veziroglu N. From hydrogen economy to hydrogen civilization. Int J Hydrogen Energy 2001;26:909–15.
[3] Biofuels ethanol for sustainable transportation. DOE/GO-10099-736, <www.energy.gov>; 1999.
[4] Scharlemann Jörn PW, Laurance WF. How green are biofuels? Science January 2008;319(4).
[5] Wang M. Development and use of GREET 1.6 fuel-cycle model for transportation fuels and vehicle technologies. Tech. report no. ANL/ESD/TM-163. Argonne National Laboratory, Center for Transportation Research; 2001.
[6] Ceccon P, Coiutti C, Giovanardi R. Energy balance of four farming systems in North-Eastern Italy. Ital J Agron 2002;6(1):73–83.
[7] <http://www.ilcorn.org/Ethanol/Ethan_Studies/Ethan_Energy_Bal/ethan_energy_bal.html>.
[8] Rossi N. Production of bioethanol for transport applications: the Italian case. MS thesis, Politecnico di Milano; 2006.
[9] Renewable Fuels Association. Fuel ethanol industry guidelines, specifications, and procedures. RFA Publication # 960501; 2003.
[10] Deluga GA, Salge JR, Schmidt LD, Verykios XE. Renewable hydrogen from ethanol by autothermal reforming. Science 2004;33:993–7.
[11] Ni M, Leung D, Leung M. A review on reforming bio-ethanol for hydrogen production. Int J Hydrogen Energy 2007;32:3238–47.
[12] Liguras DK, Kondarides DI, Verykios XE. Production of hydrogen for fuel cells by steam reforming of ethanol over supported noble metal catalysts. Appl Catal B Environ 2003;43:345–54.
[13] Perna A. Hydrogen from ethanol: theoretical optimization of a PEMFC system integrated with a steam reforming processor. Int J Hydrogen Energy 2007;32.
[14] Shu J, Grandjean BPA, Van Neste A, Kalaguine S. Catalytic palladium-based membrane reactors: a review. Can J Chem Eng 1991;69:1036–60.
[15] Armor JN. Applications of catalytic inorganic membrane reactors to refinery products. J Membr Sci 1998;147:217–33.
[16] Kikuchi E. Membrane reactor application to hydrogen production. Catal Tod 2000;56:97–101.
[17] Basile A, Gallucci F, Tosti S. Synthesis, characterization and applications of palladium membranes. In: Malada R, Menendez M, editors. Inorganic membranes: synthesis, characterization and applications. Elsevier, 2008, [chapter 8]. ISBN 978-0-444-53070-7.
[18] Tosti S, Bettinali L. Diffusion bonding of Pd–Ag membranes. J Mater Sci 2004;39:3041–6.
[19] Tosti S, Bettinali L, Lecci D, Violante V, Marini F. Method of bonding thin foils made of metal alloys selectively permeable to hydrogen, particularly providing membrane devices, and apparatus for carrying out the same. Eur Patent EP 1184125; 2001.
[20] Tosti S, Basile A, Bettinali L, Borgognoni F, Chiaravalloti F, Gallucci F. Long-term tests of Pd–Ag thin wall permeator tube. J Membrane Sci 2006;284:393–7.
[21] Tosti S, Basile A, Bettinali L, Borgognoni F, Gallucci F, Rizzello C. Design and process study of Pd membrane reactors. Int J Hydrogen Energy 2008. doi:10.1016/j.ijhydene.2008.05.031.
[22] Wanat EC, Venkataraman K, Schmidt LD. Steam reforming and water–gas shift of ethanol on Rh and Rh–Ce catalysts in a catalytic wall reactor. Appl Catal A Gen 2004;276:55–62.
[23] Vasudeva K, Mitra N, Umasankar P, Dhingra SC. Steam reforming for hydrogen production: thermodynamic analysis. Int J Hydrogen Energy 1996;21:13–8.
[24] Mas V, Kipreos R, Amadeo N, Laborde M. Thermodynamic analysis of ethanol/water system with the stoichiometric method V. Int J Hydrogen Energy 2006;31:21–8.
[25] Fort D, Harris IR. The physical properties of some palladium alloy hydrogen diffusion membrane materials. J Less Common Met 1975;41:313–27.
[26] Tosti S, Adrover A, Basile A, Camilli V, Chiappetta G, Violante V. Characterization of thin wall Pd–Ag rolled membranes. Int J Hydrogen Energy 2003;28:105–12.
[27] Tosti S. Supported and laminated Pd-based metallic membranes. Int J Hydrogen Energy 2003;28:1455–64.
[28] Macchi E, Bombarda P, Chiesa P, Consonni S, Lozza G. Gas-turbine-based advanced cycles for power generation part B: performance analysis of selected configurations. In: International gas turbine conference – Yokohama 1991, vol. 91-IGTC-72; 1991.
[29] Macchi E, Consonni S, Lozza G, Chiesa P. An assessment of the thermodynamic performance of mixed gas–steam cycles: part A – intercooled and steam-injected cycles. ASME J Eng Gas Turbines Power 1995;117:489–98.
[30] Chiesa P, Consonni S, Kreutz T, Williams R. Co-production of hydrogen, electricity and CO_2 from coal with commercially ready technology. Part A. Performance and emissions. Int J Hydrogen Energy 2005;30:747–67.
[31] Consonni S, Lozza G, Macchi E, Chiesa P, Bombarda P. Gas-turbine-based advanced cycles for power generation part A: calculation model. In: International gas turbine conference – Yokohama 1991, vol. III; 1991. p. 201–10.
[32] Campanari S, Macchi E. Thermodynamic analysis of advanced power cycles based upon solid oxide fuel cells, gas turbines and Rankine bottoming cycles. ASME paper 98-GT-585; 1998.
[33] Campanari S, Iora P, Macchi E, Silva P. Thermodynamic analysis of integrated MCFC/gas turbine cycles for multi-MW scale power generation. ASME J Fuel Cell Sci Technol 2007;4:308–16.
[34] Campanari S, Manzolini G, Beretti A, Wollrab U. Analysis of turbocharged PEM fuel cell systems for civil aircraft onboard power production. J Eng Gas Turbines Power 2008;130.
[35] Manzolini G. Membrane reactors for hydrogen separation applied to electricity production from natural gas. Ph.D. thesis, Politecnico di Milano; 2007.
[36] Larminie J, Dicks A. Fuel cell systems explained. Wiley; February 2001.
[37] Campanari S, Macchi E, Manzolini G. Innovative membrane reformer for hydrogen production applied to PEM micro-cogeneration: simulation model and thermodynamic analysis. Int J Hydrogen Energy 2008;33–34:1361–73.
[38] Personal communications with Nuvera; May 2006.
[39] Nuvera. Available from: <http://www.nuvera.com/markets/avanti.php>.
[40] Brambilla M, Mazzucchelli G. Fuel cell with cooling system based on direct injection of liquid water. Patent US6835477; 2004.
[41] Antoniazzi AB, Haasz AA, Stangeby PC. The effect of adsorbed carbon and sulfur on hydrogen permeation through palladium. J Nucl Mater 1989;162–164:1065–70.
[42] Musket RG. Effects of contamination on the interaction of hydrogen gas with palladium: a review. J Less Common Met 1976;45:173–83.
[43] Francesconi J, Mussati M, Mato R, Aguirre P. Analysis of the energy efficiency of an integrated ethanol processor for PEM fuel cell systems. J Power Sources 2007;167:151–61.